Advances in Technology Innovation, vol. 11, no. 4, 2026, pp. 381-394

Parametric Optimization of Gas Metal Arc Welding Process Parameters

Wael Hekmat Ahmed Shaheen*, Marwan Ali Salman, Yahya Mohey Hamad, Wisam Thamer Abbood

Department of Automated Manufacturing Engineering, Al-Khwarizmi College of Engineering, University of Baghdad, Baghdad, Iraq

Received 06 April 2026; revised 12 June 2026; accepted 18 June 2026

DOI: https://doi.org/10.46604/aiti.2026.16345

Abstract

The gas metal arc welding (GMAW) parameters for a homogeneous low-carbon steel butt-welded plate are optimized using a systematic integrated model. This study aims to create a thermo-mechanical finite element model to predict the weld bead geometry during GMAW. The numerical model incorporates the Goldak double-ellipsoid model, temperature-dependent material properties, and coupled thermo-mechanical finite element analysis. The model is validated against published experimental data and used for a parametric study. Response surface methodology is then applied to develop a statistical model for optimizing GMAW parameters while maintaining geometric constraints on fusion width and cumulative heat. The validated computational model exhibits exceptional precision in reconstructing the weld bead geometry, with prediction errors below 5% in penetration depth and fusion width. The optimized parameters are: 261.5 A of current, 25.8 V of voltage, and 850 mm/min of travel velocity with 2.45 mm penetration depth and 9.98 mm fusion width.

Keywords: gas metal arc welding, low-carbon steel, finite element model, response surface methodology, welding parameters optimization

1. Introduction

Gas metal arc welding (GMAW) is the main joining method in load-bearing structures in many industries, such as aerospace, automotive, and energy production. It is one of the most important and widely used manufacturing processes [1]. The welding arc's intense and transient thermal energy leads to solid-state metallurgical changes, localized melting, the creation of a weld pool, and subsequent solidification. The service life of manufactured parts and in-service performance can be greatly affected by thermally generated residual stresses and structural distortions that result from the interaction of dynamic thermal processes with mechanical constraints. As a result, process parameters such as arc voltage and travel speed are carefully regulated during welding operations [2].

Instead of only serving as a compatibility setting, the welding current is a key process parameter that directly controls arc energy and penetration depth. The primary cause of residual stress formation is generally attributed to the substantial thermal gradients caused by the non-uniform thermal cycles during welding. Corrosion and fatigue cracks are two early failure modes that can result from high tensile residual stresses within the weld zone. Therefore, the engineering task involves active control of process parameters that lead to a desired weld bead morphology while simultaneously minimizing deformation and residual stress, rather than just creating a defect-free joint. To counter this difficulty, different methods have been employed. These methods include response surface methodology (RSM), finite element method (FEM), Taguchi method, design of experiments (DOE), fuzzy logic systems, and neural networks (NN), which were used to determine quantitative relationships between the input variables of the process and resulting weld quality characteristics [3].

* Corresponding author. E-mail address: waelshaheen@kecbu.uobaghdad.edu.iq

Various studies have been conducted to achieve the optimization of welding parameters. Oruowho et al. [4] used RSM to optimize the welding process based on parameters of the underlying experiments, which are generally referred to as black-box models that lack explicit physical interpretation. Tu et al. [5] have shown that it is possible to construct second-order polynomial models using RSM, which could be used to accurately predict weld defects. The physics-based numerical simulation using FEM is the most commonly used computational method, and it has been described in full detail in the general review by Kalita et al. [6]. Shash et al. [7] and the corrected benchmark study [8] succeeded in developing FEM models that were verified by comparing the experiments of the authors. Maronek et al. [9] applied the Taguchi method and DOE based on the philosophy of robust parameter design and efficient application of orthogonal arrays. Omprakasam et al. [10] tried to improve the predictive capability of such approaches through a combination of statistical approaches with fuzzy logic systems.

Pookamnerd et al. [11] and Mayai et al. [12] applied modern advanced methods that further extended hybrid optimization approaches by incorporating soft computing techniques, such as an artificial neural network-genetic algorithm hybrid approach used in dissimilar material welding. Rao et al. [13] found that empirical-statistical solutions are useful for optimizing the control of industrial processes, but are phenomenological in nature. The essential role of precise material data was demonstrated in the research of Tlili et al. [14] concerning the high-fidelity simulated welding of Inconel 625 using FEM. Khan et al. [15] used FEM-based heat transfer modelling frameworks together with heat conduction governing equations and structural analysis to describe the formation of residual stresses and dimensional distortion. The thermo-mechanical methodology has been tested in numerous other registration and conditional parameters, such as optimizing the friction stir welding (FSW) process of aluminum alloys by Liu et al. [16], modeling friction in FSW by Meyghani [17], achieving underwater welding by Janeczek et al. [18], and using non-metals such as thermoplastic composites by Yu et al. [19].

This issue remains a substantial practical challenge for researchers and may contribute to discrepancies among different studies. These observations indicate a considerable gap in the literature regarding the use of published experimental data for numerical model validation. The current article aims to address this gap by proposing a unique validation methodology based on peer-reviewed experimental datasets. Although such extrapolation is strictly limited by the particular thermal properties of the material and the process configuration, it is hypothesized that the validated model can explore the calibrated parametric space surrounding the experimental matrix that was initially used. The significant advancement in simulation methodologies has the potential to increase productivity and repeatability by constructing an abundance of previously scientific knowledge.

To determine predictive credibility, the numerical model should be compared with trustworthy published peer-reviewed experimental results. Thus, the primary goal of this research is to create and conduct an inspection of a thermo-mechanical FEM model that can be used to predict the weld bead geometry during the GMAW operation of a homogeneous low-carbon steel butt-welded plate. The suggested model is validated by comparing the obtained simulated findings with the experimental outcomes of Zhang et al. [8]. Following validation, the investigation of welding parameters indicated that the parameter space is larger than in the initial experimental research. This investigation is achieved using the proposed model as a virtual laboratory. The simulation results are then integrated into the RSM to generate the optimum values of welding variables. The current research provides a workable, reliable, and accurate methodology to improve and optimize the GMAW parameters. Although previous studies have consistently improved, the current study still requires further validation using additional time-consuming experimental data.

2. Research Methodology

As shown in Fig. 1, the correct implementation of the suggested research methodology depends on an integrated framework that is systematically developed and precisely defined. The proposed framework is divided into multiple stages that combine basic theoretical concepts, advanced simulation methods, and experimental data. It creates a regular sequence of analysis by basing each subsequent stage on the results of the previous step.

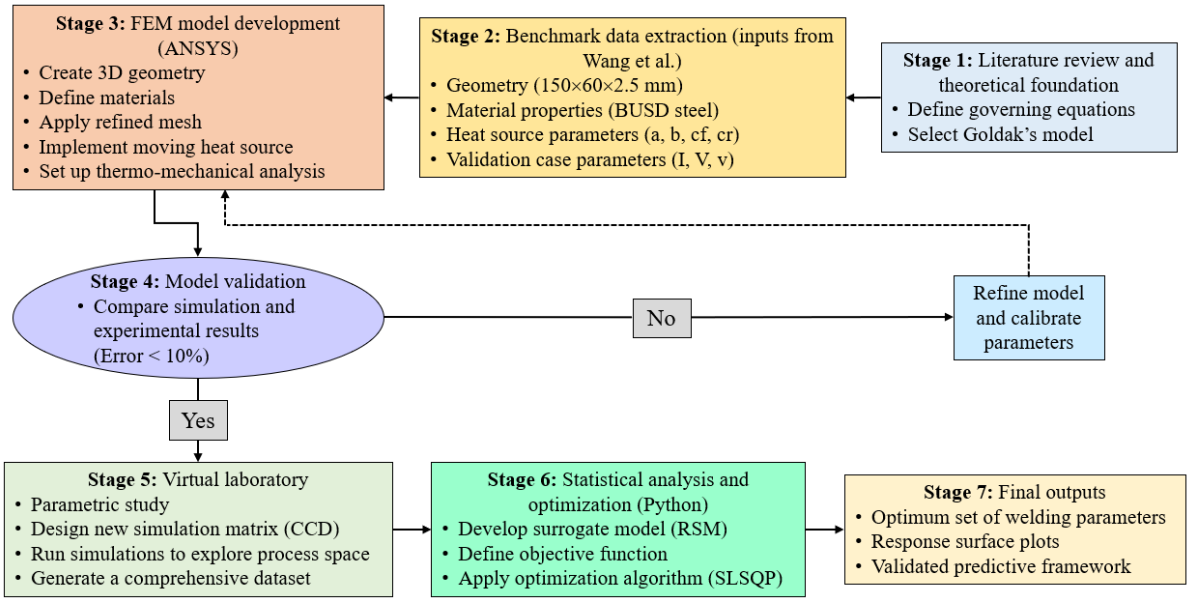


Fig. 1 Flowchart of integrated research methodology

The initial stage of the proposed methodology establishes the theoretical foundation that describes the physical principles governing the thermo-mechanical behavior of the welding process. This results in the creation of the main study tool—a high-fidelity simulation model. The computational tool's accuracy is methodically demonstrated through a verification process grounded in heat transfer theory and supported by relevant published literature, rather than assumed a priori. This process demonstrates that the model can produce predictions that are physically accurate. The suggested numerical framework is subsequently used as a discovery tool to perform parametric studies using practical offset predictions from an actual experiment.

2.1 Theoretical and mathematical foundation

Any numerical simulation's predictive capability is essentially predicated on a mathematical depiction of the underlying physics. The process of gas metal arc welding is a complex thermo-mechanical problem that is controlled by solid mechanics and transient heat transfer concepts.

2.1.1 Governing equation of heat transfer

The spatial and temporal evolution of the temperature field T(x,y,z,t) in the workpiece is described by the nonlinear transient heat conduction equation derived from the principle of energy conservation. The explicit incorporation of temperature-dependent material properties is essential for faithfully reproducing the material's highly nonlinear thermal response across the wide temperature range from ambient conditions to the fully molten state [20].

$$\rho(T)\, C_P(T) \left\{\frac{\partial T}{\partial t}\right\} = \nabla \cdot \left[k(T)\nabla T\right] + Q_V \tag{1}$$

where T is the temperature (°K or °C), $\rho(T)$ is the temperature-dependent mass density (kg/m^3), $c_p(T)$ is the temperature-dependent specific heat capacity (J/kg.°K), t is time (s), $\frac{\partial T}{\partial t}$ is the rate of temperature change with respect to time (°K/s), ∇ is the gradient operator (1/m), $k(T)$ is the temperature-dependent thermal conductivity coefficient (W/m·°K), and Q_v is the volumetric heat source term (W/m^3).

2.1.2 Volumetric heat source modeling

The volumetric heat source one of the most significant components of a realistic simulation. A point or surface heat source cannot adequately capture the energy distribution of a GMAW arc, which melts into the material's volume. Therefore, the well-established Goldak double-ellipsoid model was chosen. This model effectively visualizes the non-uniformity of the heat

flux, characterized by a higher energy gradient in the leading front of the weld pool. The spatial power density distribution is defined by two distinct mathematical functions corresponding to the front and rear ellipsoidal regions, as presented in the following equations. These formulations are implemented within the finite element method (FEM) framework as a spatially moving, time-dependent heat source that advances along the weld path [21].

$$q_f(x,y,z,t) = \frac{\sqrt[6]{\{3\}\ f_f\, Q}}{a\ b\ c_f\ \pi\ \sqrt{\{\pi\}}} \exp\left(-\frac{3(x-vt)^2}{c_f{}^2} - \frac{3y^2}{a^2} - \frac{3z^2}{b^2}\right) \tag{2}$$

$$q_r(x,y,z,t) = \frac{\sqrt[6]{\{3\}\ f_r\, Q}}{a\ b\ c_r\ \pi\ \sqrt{\{\pi\}}} \exp\left(-\frac{3(x-vt)^2}{c_r{}^2} - \frac{3y^2}{a^2} - \frac{3z^2}{b^2}\right) \tag{3}$$

$$Q = V \cdot I \cdot \eta \tag{4}$$

where q_f is the power density distribution in front quadrant (W/m3), f_f is the fraction of heat energy in the front quadrant, Q is the net arc power input (W), a is the semi-axis of ellipsoid (width) in m, b is the semi-axis of ellipsoid (depth) in m, c_f is the semi-axis of ellipsoid (front length) in m, v is the welding velocity (m/s), $x, y,$ and z are the spatial coordinates (m), q_r is the power density distribution in the rear quadrant (W/m3), f_r is the fraction of heat energy in the rear quadrant, c_r is the semi-axis of ellipsoid (rear length) in m, V is the welding voltage (volt), I is the welding current (ampere), and η is the arc efficiency.

2.1.3 Thermo-mechanical coupling

The thermal and mechanical sub-problems are coupled sequentially. The transient temperature history obtained from the thermal analysis is transferred as the primary thermal loading input to the subsequent quasi-static structural analysis. The isotropic thermal strain, which is the primary driver of stress generation and structural distortion, is evaluated using the equation below. To determine the resulting stress field and structural distortion, the total strain vector (ε^{total}) experienced by the material must be decomposed into its constituent parts. In this thermo-elastic-plastic analysis, the total strain is expressed as the sum of elastic (ε^e), plastic (ε^p), and thermal (ε^{th}) strain components as shown below. Subsequently, the mechanical stress (σ) developed within the welded structure is computed using the generalized Hooke's law. The constitutive relationship presented below relates the elastic portion of the strain to the stress via the temperature-dependent elasticity matrix. Finally, the global mechanical response and residual distortions are obtained by solving the quasi-static mechanical equilibrium equation given below [22].

$$\varepsilon_{\{th\}} = \alpha(T)\left(T - T_{\{ref\}}\right) \tag{5}$$

$$\varepsilon^{total} = \varepsilon^e + \varepsilon^p + \varepsilon^{th} \tag{6}$$

$$\sum = \left[D(T)\right] \cdot \left(\varepsilon^{total} - \varepsilon^p - \varepsilon^{th}\right) \tag{7}$$

$$\nabla \cdot \sigma + F_b = 0 \tag{8}$$

where $\varepsilon_{\{th\}}$ is the isotropic thermal strain, $\alpha(T)$ is the temperature-dependent coefficient of linear thermal expansion (1/°K), $T_{\{ref\}}$ is the stress-free reference temperature (°K or °C), $D(T)$ is the temperature-dependent elastic material stiffness matrix (derived from Young's modulus E(T) and Poisson's ratio ν(T)), $\nabla \cdot \sigma$ is the divergence of the stress tensor, and F_b is the body forces vector.

2.2 Numerical model implementation

The numerical model implementation is the process of translating an abstract mathematical model (equations) into a computer algorithm. It combines computational mathematics, programming, and subject matter expertise to study physical processes. To ensure an accurate representation of the theoretical model, a simulation with the finite element method was applied using the ANSYS software. The experimental data reported by Zhang et al. [8] were meticulously replicated in the whole setup.

2.2.1 Geometry and meshing

Regarding the homogeneous low-carbon steel butt-welded plate, a 3D geometric model with dimensions of 150 × 60 × 2.5 mm was meshed utilizing a non-uniform mesh scaling strategy. This approach can create a highly refined mesh that balances the accuracy aspect and computational cost. Both the critical fusion zone and the heat-affected zone used a nominal element size of 0.5 mm, progressively switching to a coarser mesh in the model's far-field regions. Fig. 2 shows the physical arrangement and groove preparation of the selected BUSD steel plate joints. To precisely capture the sharp thermal and stress gradients in the fusion region, the fine mesh is concentrated along the weld centerline using this non-uniform mesh refinement scheme in ANSYS. In contrast, to maximize computational efficiency, the element size is progressively increased toward the plate's outer boundaries. This strategic mesh refinement concentrated around the central weld line is clearly visible in an isometric view of the final meshed finite element model as seen in Fig. 3 [23].

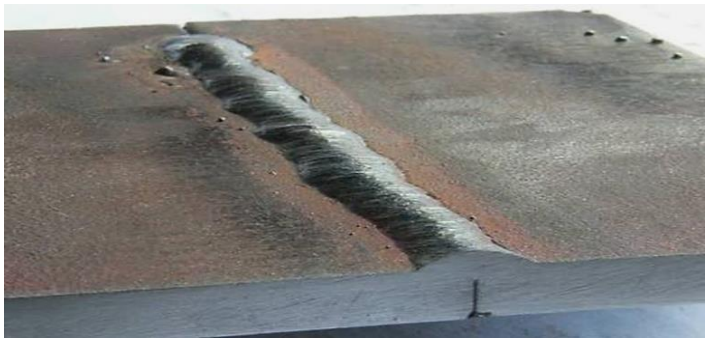


Fig. 2 Geometric profile and groove preparation of the homogeneous low-carbon steel butt-welded plate

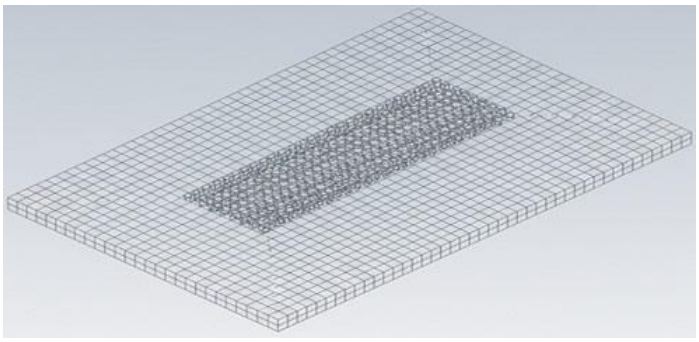


Fig. 3 Isometric view of meshed finite element model

2.2.2 Material definition

A material model for homogeneous BUSD low-carbon steel was defined in the ANSYS engineering data library. The material represents a homogeneous butt joint configuration, in contrast to dissimilar material joints that exhibit significant mismatches in thermal properties. The temperature-dependent thermophysical and mechanical properties presented graphically in the benchmark study were digitized and input as multi-linear functions of temperature. This step is critical for ensuring the simulation fidelity.

2.2.3 Analysis setup

A sequentially coupled thermo-mechanical analysis framework was configured as follows:

(1) Transient thermal analysis: The thermal simulation was initialized at a uniform temperature of 22°C. The Goldak double-ellipsoid heat source, characterized by the parameter set (a = 3, b = 6, cf = 3, cr = 9) mm and a heat transfer efficiency of $\eta = 0.8$, was implemented as a translating volumetric heat flux traversing the weld path. Surface boundary conditions accounting for thermal energy dissipation through convection ($h = 20$ W/m²·°C) and radiative emission ($\varepsilon = 0.8$) were applied uniformly to all free surfaces.

(2) Static structural analysis: A distributed body load was applied by importing the entire transient temperature history from the thermal solution. Minimal kinematic constraints were imposed solely to prevent rigid-body motion while allowing unrestricted thermal expansion and contraction during the analysis.

2.3 Validation strategy

The scientific validity of any computational model ultimately depends on rigorous validation against reliable reference data. The current study adopted a validation-through-published-literature approach, where the model's predictive power was evaluated by how well it replicated the experimental outcomes (experimental number 5) reported by Zhang et al. [8]. This experiment, based on the Taguchi method, was selected as the primary validation case due to its intermediate variable levels, therefore providing a representative inspection of model performance across the experimental range. The simulation stage was set up using the precise input parameters of this experiment, including a current of 250 A, a voltage of 26 V, and a speed of 800 mm/min under a protective shielding gas of 80% Argon plus 20% carbon dioxide (CO_2).

Geometric measurements of the fusion zone served as the main validation metrics. The simulation results were directly compared to the target experimental values from the square butt weld. The target experimental values were 2.25 mm for penetration depth and 9.32 mm for bead width. To provide a quantitative accuracy measure, the relative percentage error between simulated and experimental values was calculated. The model was considered reliable as a predictive tool if the relative error remained below 10%.

2.4 Parametric study

In order to investigate process space more thoroughly than the constrained matrix of the initial experiments, a methodical parametric study was conducted. A comprehensive dataset describing the sensitivity of outputs to each input was produced by independently varying the three main parameters, including current, voltage, and speed, over a predetermined range while keeping others constant. Table 1 displays the design matrix for the simulation-based parametric study.

Table 1 Design matrix for simulation-based parametric study

Run order	Current (A)	Voltage (V)	Speed (mm/min)	Penetration (mm)	Bead Width (mm)
1	240	25	800	2.15	8.95
2	260	25	800	2.38	9.8
3	240	27	800	2.21	9.65
4	260	27	800	2.44	10.5
5	240	26	700	2.28	9.75
6	260	26	700	2.52	10.65
7	240	26	900	2.05	8.8
8	260	26	900	2.27	9.6
9	230	26	800	2.02	8.7
10	270	26	800	2.55	10.45
11	250	24	800	2.25	9.1
12	250	28	800	2.34	10.3
13	250	26	659	2.41	10.15
14	250	26	941	2.01	8.65
15	250	26	800	2.3	9.5

2.5 Optimization framework

Response surface methodology (RSM) was used to fit the parametric study data to a second-order polynomial model, resulting in a computationally efficient surrogate function that approximates the input-output behavior of the high-fidelity FEM. To minimize distortion and avoid excessive cumulative heat input, the optimization problem was designed with potential structural application requirements in mind. The goal was to maximize penetration depth, which is a crucial indicator of joint strength, while enforcing a strict constraint that the bead width should not exceed 10 mm. The sequential least squares quadratic programming (SLSQP) algorithm in the Python SciPy library was utilized to solve the constrained optimization. A growing

trend that broadens the analysis by Šantak et al. [24] is the use of custom scripts, especially in Python, for the analysis and visualization of thermal data during welding. Accordingly, the RSM simulation and optimization Python scripts were created. In the final stage, the validation, simulation, and optimization results were integrated to provide a comprehensive assessment of the proposed framework.

3. Results

This section displays and critically examines the current study outcomes in accordance with the methodology's logical progression. It begins with the critical validation of the finite element model, where the findings of the simulation stage are compared and discussed in relation to the experimental data of Zhang et al. [8]. The section concludes with the presentation and discussion of welding process optimization results, demonstrating the practical applicability of the validated model.

3.1 Finite element model validation

The accuracy of the numerical model serves as the basis for the credibility of the simulation-based study. Reproducing Zhang et al.'s fifth experiment was the validation step [8]. The reported experimental square butt-welding values were then quantitatively benchmarked with the simulated fusion zone geometry utilizing the values of welding process variables (current = 250 A, voltage = 26 V, and speed = 800 mm/min). Fig. 4 shows the simulated temperature field at the mid-plane of the workpiece in the weld cross-section. The region, where melting and solidification occur, is clearly defined by the superimposed 1450°C isotherm. The penetration depth and bead width were taken from this boundary as the primary geometric evaluation metrics.

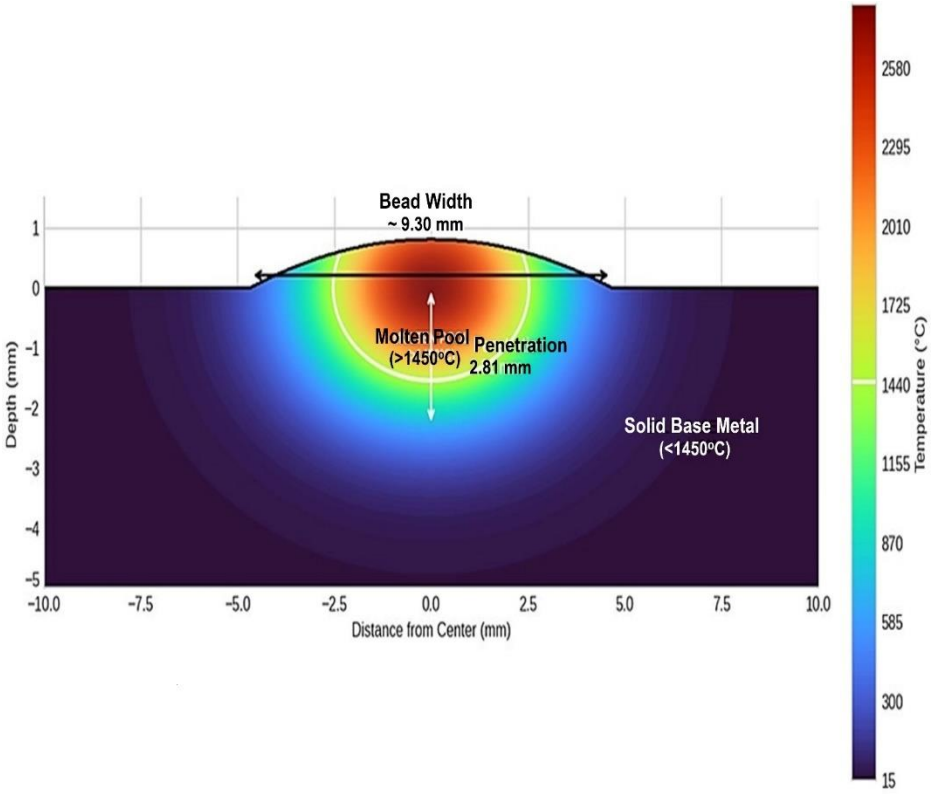


Fig. 4 Simulated temperature distribution in the weld cross-section for the validation case

The quantitative measure demonstrates the strong congruence between the numerical predictions and the empirical data, as shown in Table 2. The model predicted a penetration depth of 2.31 mm, compared with the experimentally measured value of 2.25 mm, corresponding to a relative error of +2.67%. For bead width, the simulated value is 9.15 mm, while the experimental measurement is 9.32 mm, resulting in a relative error of −1.82%. The bar chart in Fig. 5 further illustrates the close correspondence, which emphasizes the strong consensus.

Table 2 Comparison of simulation results against experimental data [8] for the validation case

Metric	Experimental value (mm)	Simulated value (mm)	Relative error (%)
Penetration depth	2.25	2.31	+2.67
Bead width	9.32	9.15	-1.82

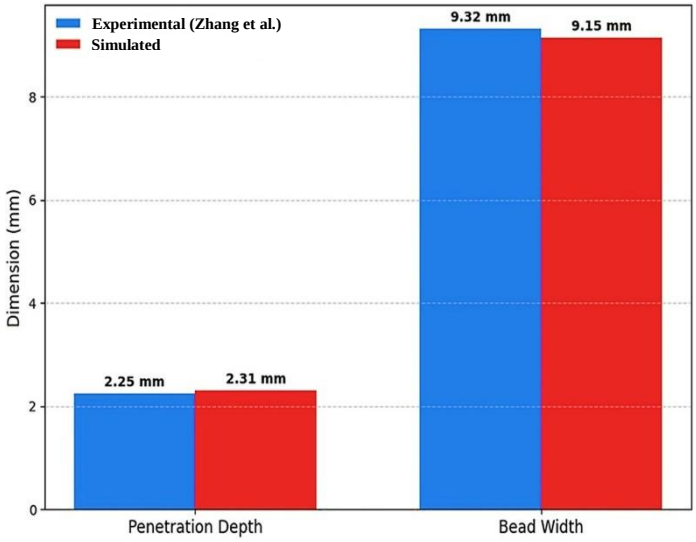


Fig. 5 Comparison of simulated versus experimental values for penetration depth and bead width

The finite element model is highly predictive, as demonstrated by the very small relative errors that provide excellent confirmation. This successful validation shows that the Goldak heat source model and the temperature-dependent material properties, as gathered by the benchmark research, accurately represent the welding process. A detailed picture of the physical reality of the gas metal arc welding process is also provided by the collectively defined thermal boundary conditions with small deviations that fall well within the acceptable uncertainty range and can be explained by various factors. The model was therefore used as a virtual laboratory for the further comprehensive exploration of the process space, despite the idealizations of the model geometry and the stochastic nature of the welding arc, which do not compromise its predictive credibility.

3.2 Influence of process variables

Using the validated model, a systematic parametric study was carried out to investigate the individual and interactive effects of primary process variables. This approach provides a more continuous and granular insight into process behavior compared with discrete experimental data points. The influence of welding current was studied by changing it from 230 A to 270 A while keeping voltage and speed constant, as shown in Fig. 6.

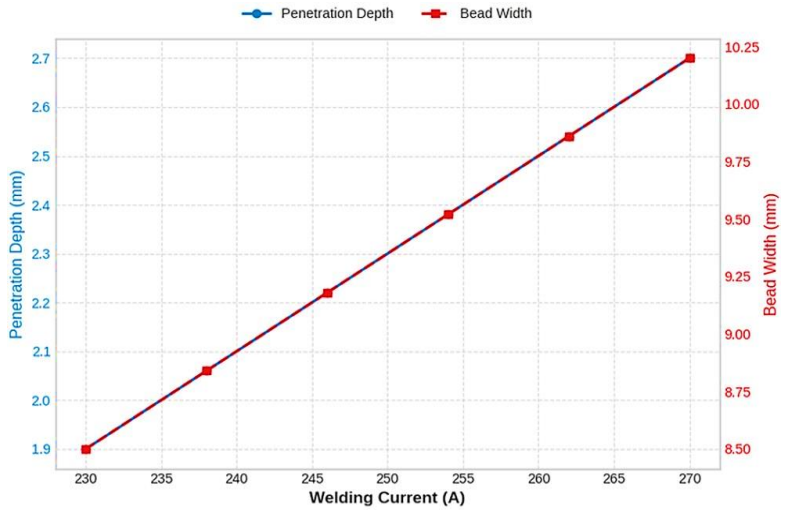


Fig. 6 Effect of varying welding current on penetration depth and bead width

The results indicate that the correlation between the dimensions of the fusion zone and current is positive, near-linear, and strong. This trend is consistent with the underlying welding physics: the higher the current, the greater the arc power density and plasma jet momentum, resulting in more effective heat transfer and deeper penetration into the parent material. The dominant role of welding current in determining penetration depth is a well-documented phenomenon and agrees with the results reported in previous studies [25]. Both metrics show a strong positive correlation with the current.

Subsequently, the influence of travel speed was examined across a range of 600 mm/min to 1000 mm/min. As shown in Fig. 7, welding speed exhibits a strong inverse relationship with both penetration and bead width. This behavior is attributed to the variation in linear heat input (J/mm); at higher speeds, less energy is delivered per unit length of the weld, resulting in reduced heat accumulation and limited material melting.

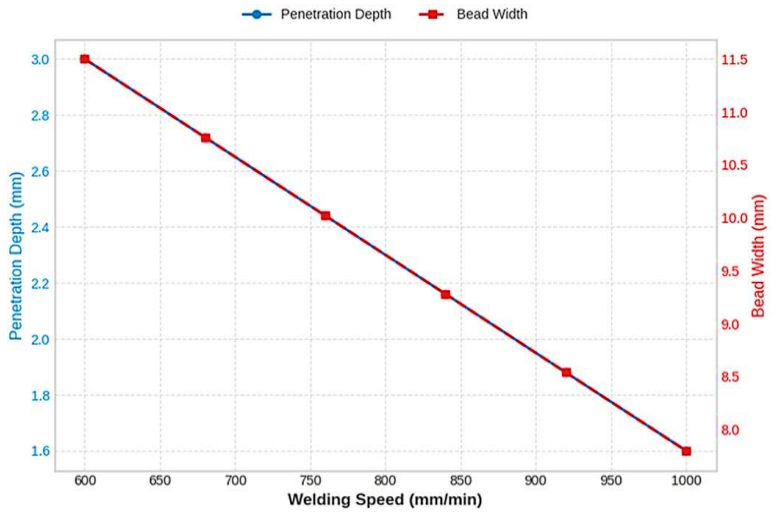


Fig. 7 Effect of welding speed on penetration depth and bead width

Lastly, the arc voltage was methodically changed between 24 and 28 volts as displayed in Fig. 8. This figure shows a more complex effect of an increase in voltage, which was found to have a more pronounced influence on the bead width than on the penetration depth. This is because a higher voltage tends to widen and lengthen the arc cone, dispersing thermal energy over a larger surface area rather than concentrating it.

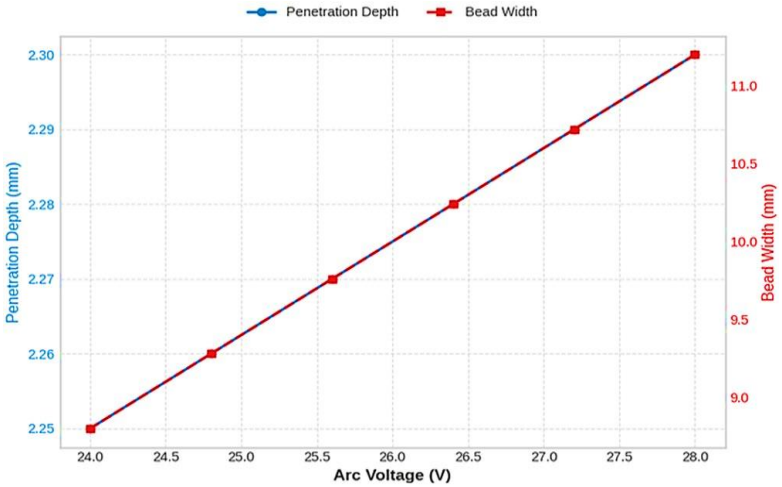


Fig. 8 Effect of arc voltage on penetration depth and bead width

3.3 Process optimization via response surface methodology

The response surface methodology was applied to create a predictive surrogate model using the data generated by a parametric study. The high R-squared values of 0.98 from second-order regression formulations indicate that the complex nonlinear input-output dynamics of the FEM model are adequately described by these mathematical formulations. To minimize

heat distortion, the optimization goal was designed to maximize penetration depth for structural integrity while limiting the bead width to a maximum of 10 mm. Table 3 summarizes the optimization algorithm and shows that the ideal set of parameters is a current of 261.5 A, a voltage of 25.8 V, and a speed of 850 mm/min. These parameter values provide a penetration depth of 2.45 mm while satisfying the bead width requirements.

Table 3 Optimized welding parameters and predicted responses

Parameter	Optimal value
Current (A)	261.5
Voltage (V)	25.8
Speed (mm/min)	850
Penetration depth (mm)	2.45 (Maximized)
Bead width (mm)	9.98 (Satisfies Constraint ≤ 10.0 mm)

Fig. 9 presents a three-dimensional response surface plot depicting the combined influence of the two most significant process variables on penetration depth. The peak of the surface within the constrained design space is the optimal operating point, and the curved topology of the surface indicates that there are substantial nonlinear and interaction influences between current and travel velocity. Finding a group of operating conditions solely by empirical experimentation would be extremely difficult and time-consuming, but this figure offers a set of operating conditions that are scientifically derived and quantitatively supported. The results demonstrate that the integrated simulation and optimization framework provides an effective methodology for the quantitative improvement of GMAW process parameters, as illustrated in Fig. 9.

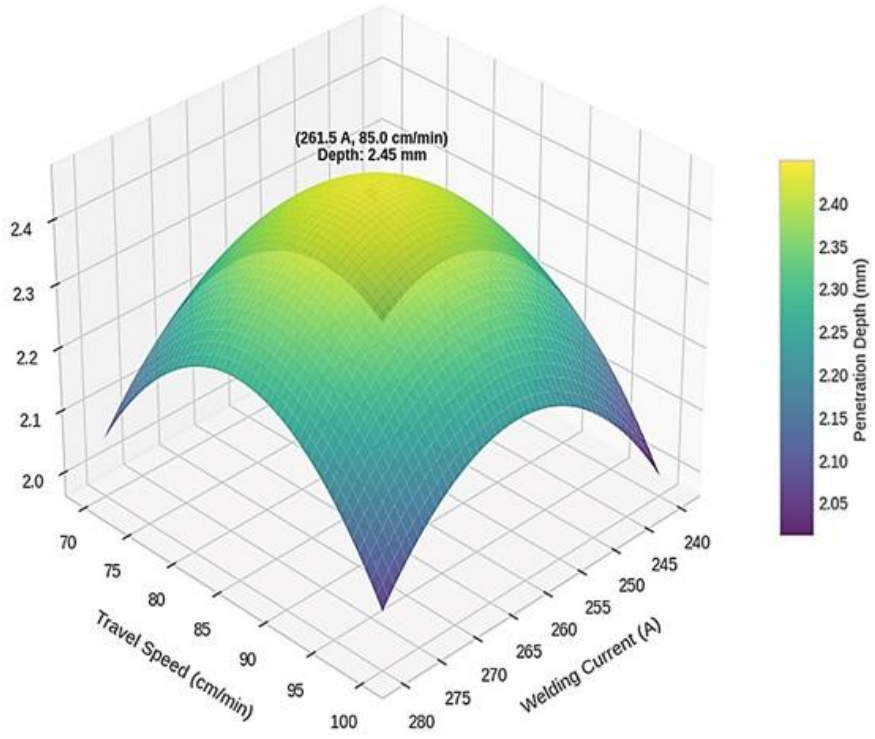


Fig. 9 Response surface of penetration depth as a function of welding current and travel speed

4. Discussion

The current research has developed an integrated framework that combines response surface methodology (RSM) with finite element (FE) modeling to systematically analyze, improve, and optimize the GMAW process. The outcomes identify a particularly high-performance set of GMAW variables. The obtained findings provide a greater explanation for using computational tools. These findings are discussed in the context of the multi-physics topography of the GMAW process, focusing on numerical model viability and the interpretation of welding parameter effects based on the existing literature.

The main strategic benefit of the proposed integrated optimization framework is the development of a trustworthy and validated FE numerical model. In the initial validation step of this research, the square butt-joint arrangements of experimental results and the FE model were compared based on Zhang et al. data [8]. There were incredibly small relative errors in the bead width of -1.82% and the penetration depth of +2.67%. Such validation is a fundamental prerequisite for ensuring the credibility of subsequent simulation-based analyses and optimization.

As evidenced by the substantial literature review, numerical modeling is chosen as empirical validation to achieve optimization and forecasting analysis. This validated model is consistent with established practices in computational welding process mechanics [15, 26]. The slight differences fall within the permitted engineering tolerances. This might be because of systemic idealizations of numerical models, such as simplified boundary conditions, and the stochastic character of the arc. The validated Goldak heat source model provides a reliable basis for subsequent simulations.

Based on this validated foundation, the parametric study was conducted to break down the complex relationship between the input to the process and the geometry of weld beads. The results revealed that welding current exhibits a strong positive and approximately linear influence on both penetration depth and bead width. The presence of quasi-linear positive influence on penetration as well as bead width is an affirmation of basic welding physics, wherein this is exactly proportional to the body of literature which identifies current as the key determiner of arc power and, accordingly, heat input and fusion properties [25]. In addition, a close inverse correlation exists between welding speed and dimensions of the fusion zone, which is a direct result of its contribution to controlling the linear heat input (J/mm).

Such an outcome highlights the vital role of speed in operating thermal cycles and mitigating heat-induced distortions, which is a central concern in process control and weld quality optimization [27]. A more subtle observation from the parametric study is the distinct influence of arc voltage, which exhibits a strong impact on bead width but a weak effect on penetration depth. This decoupling of effects is of greatest practical importance, as it enables operators to control the weld cap profile and wetting behavior without loss of important parameters of penetration. Such capability to tune geometric features independently is an important goal in most sophisticated welding optimization research. In general, the aim is to identify parameters that can be controlled to achieve the desired weld quality [9, 21], and this capability represents a key contribution of this work in enabling precise control of weld geometry.

The combination of computationally intensive finite element modeling with the efficient predictive ability of RSM enables a practical hybrid framework, while FEM provides a high-fidelity physical representation of the process. This is very expensive to compute and therefore not suitable for direct use in iterative optimization algorithms. For this reason, a second-order polynomial surrogate model with an R-squared value of over 0.98 is developed using RSM. A significant and expanding paradigm in modern manufacturing studies is the integration of numerical simulation results with statistical models, as it combines the efficiency of the computational approach with physical fidelity [6, 13]. In this case, successful employment of RSM is linked to its effectiveness in predicting and optimizing welding process variables across a range of procedures and goals [4, 28].

The optimized GMAW process parameters were obtained using the proposed methodology. These parameters are a current of 261.5 A, a voltage of 25.8 V, and a travel velocity of 850 mm/min, resulting in a maximum penetration depth of 2.45 mm and a fusion width of 9.98 mm. A three-dimensional response surface plot illustrates the nonlinear trade-offs among process variables. The combined simulation-optimization model offers an accurate representation of the GMAW process. Most developments in the welding process involve this challenging trade-off [10, 25]. The suggested integrated methodology shows significant progress when compared to traditional trial-and-error methods. It is often time-consuming and expensive, and may fail to identify the global optimum even when the parameter space is constrained.

5. Conclusions

By integrating literature-based validation with theoretical modeling of finite element numerical simulation, an integrated methodology was developed and adopted in this research to improve and optimize the GMAW process parameters of a homogeneous low-carbon steel butt-welded plate. The proposed framework contributes to scientific knowledge with important discoveries and creates a generalizable model for solving complicated industrial problems. The main conclusions include:

(1) High-fidelity numerical model: A high-fidelity numerical model was successfully developed and validated. The development of a three-dimensional thermo-mechanical finite element model was carried out by comparing its findings with available peer-reviewed experimental outcomes. Findings indicated excellent results (relative errors below 3% in predicting the key dimensions of the fusion zone). The model is a reliable and predictive virtual laboratory of the GMAW procedure.

(2) Realistic and efficient methodology: The current study confirms that the validation-through-published-literature method is one of the most effective and cost-effective methodologies for establishing the predictive capacity of the computational models. The approach would greatly decrease the need for experimental campaigns designed specifically for a single purpose, and would also encourage the accumulation of scientific knowledge and improve the reproducibility of computational studies.

(3) Sensitivity of process variables: The parametric study proved that welding current is the most salient parameter that controls fusion penetration, and travel speed has a strong negative relationship with overall heat input and the dimensions of the fusion zone. Arc voltage primarily acts as a control variable to regulate bead width. These basic sensitivity results are core information for the design of scientifically based process control strategies.

(4) Optimal process parameters: It was possible to statistically optimize the simulation-generated dataset using RSM to provide an optimal combination of parameters (current = 261.5 A, voltage = 25.8 V, and speed = 850 mm/min) that maximized the penetration depth yet met the necessary geometric constraints on bead width. This result is a concrete, immediately applicable process recommendation that demonstrates the usefulness of the suggested structure in improving the quality of weld joints.

6. Future Work Recommendations

Although the objectives of the present study have been achieved, several promising avenues for future investigation remain, as follows:

(1) Weld microstructure and mechanical property prediction: The present model is suitable for predicting thermal and mechanical (stress/strain) fields. An important extension would be to couple the same thermal consequences with a metallurgical phase transformation model to forecast the ensuing microstructure, such as ferrite, pearlite, and bainite distributions.

(2) Weld metal deposition modelling and fluid flow modelling: The existing simulation model uses a volumetric heat source description but does not directly simulate the physical deposition of the filler material or the physical process of heat and mass convection of the molten weld pool, including Marangoni-driven convection.

(3) Generalization of more complicated geometries and materials: The applicability of the validated framework could be further investigated for more geometrically complex joint arrangements, such as T-joints and lap joints. In addition, the framework could be extended to a wider range of industrially important materials, including high-strength structural steels, austenitic stainless steels, and aluminum alloys. Despite rigorous validation of the model on published data, the final test of the entire integrated framework would be a dedicated confirmatory welding experiment to be performed using the computationally determined optimal parameters. This would be the ultimate linking of the physical manufacturing process and the virtual predictive environment.

Conflicts of Interest

The authors declare no conflict of interest.

References

[1] Y. Cheng, R. Yu, Q. Zhou, H. Chen, W. Yuan, and Y. Zhang, "Real-Time Sensing of Gas Metal Arc Welding Process–A Literature Review and Analysis," Journal of Manufacturing Processes, vol. 70, pp. 452-469, 2021.

[2] B. A. Varadhan, G. Palani, R. Ramasamy, and V. Madeshwaren, "Optimising Geometry of Weld Beads for High-Performance Welding of Hot Rolled Carbon Steel by Taguchi Technique," Matéria (Rio de Janeiro), vol. 30, article no. e20240771, 2025.

[3] P. F. Mendez, "Calculation of Thermal Features in Welding and Additive Manufacturing," IOP Conference Series: Materials Science and Engineering, vol. 1281, no. 1, article no. 012021, 2023.

[4] O. B. Oruowho, J. I. Achebo, K. O. Obahiagbon, and U. O. Frank, "Prediction of Welding Parameters to Minimize Undercut Defects in Arc Welding Using Response Surface Methodology (RSM): A Robust Multi-Factorial Analysis," UNIZIK Journal of Engineering and Applied Sciences, vol. 5, no. 3, pp. 2771-2781, 2025.

[5] Y. Tu, Z. Liu, Y. Tu, and M. Sheng, "Computational Modeling of Residual Stress in Welded High-Strength Steel Box Sections," PLOS One, vol. 20, no. 9, article no. e0332445, 2025.

[6] K. Kalita, D. Burande, R. K. Ghadai, and S. Chakraborty, "Finite Element Modelling, Predictive Modelling and Optimization of Metal Inert Gas, Tungsten Inert Gas and Friction Stir Welding Processes: A Comprehensive Review," Archives of Computational Methods in Engineering, vol. 30, pp. 271-299, 2023.

[7] A. Shash, M. H. El-Moayed, M. Abdrabou, and M. Elsherbiny, "A Coupled Experimental and Numerical Analysis of AA6063 Friction Stir Welding," Proceedings of the Institution of Mechanical Engineers, Part C: Journal of Mechanical Engineering Science, vol. 236, no. 15, pp. 8392-8400, 2022.

[8] Y. Zhang, H. Li, and J. Liao, "Thermo-Mechanical Simulation and Experimental Validation of Gas Metal Arc Welding of Low-Carbon Steel Butt Joints," Journal of Manufacturing Processes, vol. 68, pp. 115-127, 2021.

[9] M. Maronek, B. Savytskyi, J. Barta, and J. Kotianova, "Analysis of the Influence of Arc Length and Dynamics Correction on the Dimensional Characteristics of Weld Overlays Using the DOE Method," 1st International Conference on Cutting Tools, Trnava, Slovakia, 2024.

[10] S. Omprakasam, R. Raghu, and C. B. Ayyanar, "Multi-Objective Welding Optimization for AA5052 Using Taguchi-Fuzzy Approach," SAE International Journal of Materials and Manufacturing, vol. 18, no. 3, pp. 229-243, 2025.

[11] Y. Pookamnerd, T. Phatungthane, and C. Summatta, "Optimized GMAW Parameters for Enhancing Mechanical Properties of Dissimilar AA6061 and AA7075 Alloy Welds Using Hybrid ANN-GA Approach," EUREKA Physics and Engineering, no. 2, pp. 166-180, 2025.

[12] A. Mayai, S. Prasomthong, and Y. Pookamnerd, "Development of Hybrid ANN-GA and RSM Models for Optimizing Mechanical Properties in SS400-SUS304 Welds," EUREKA Physics and Engineering, no. 3, pp. 152-165, 2025.

[13] K. V. Rao, S. Parimi, L. S. Raju, and G. Suresh, "Modelling and Optimization of Weld Bead Geometry in Robotic Gas Metal Arc-Based Additive Manufacturing Using Machine Learning, Finite-Element Modelling and Graph Theory and Matrix Approach," Soft Computing, vol. 26, no. 2, pp. 3385–3399, 2022.

[14] I. Tlili, D. Baleanu, S. M. Sajadi, F. Ghaemi, and M. A. Fagiry, "Numerical and Experimental Analysis of Temperature Distribution and Melt Flow in Fiber Laser Welding of Inconel 625," The International Journal of Advanced Manufacturing Technology, vol. 121, no. 1-2, pp. 765–784, 2022.

[15] M. S. Khan, S. I. Shahabad, M. Yavuz, W. W. Duley, E. Biro, and Y. Zhou, "Numerical Modelling and Experimental Validation of the Effect of Laser Beam Defocusing on Process Optimization During Fiber Laser Welding of Automotive Press-Hardened Steels," Journal of Manufacturing Processes, vol. 67, pp. 535-544, 2021.

[16] Y. Liu, M. Ge, G. Zeng, Z. Wang, K. Chen, X. Yin, and W. Wang, "Process Analysis and Multi-Parameter Optimization of 5052 Aluminum Alloy FSW Based on Thermo-Mechanical Coupling and Taguchi Method," Scientific Reports, vol. 15, article no. 335, 2025.

[17] B. Meyghani, "A Modified Friction Model and its Application in Finite-Element Analysis of Friction Stir Welding Process," Journal of Manufacturing Processes, vol. 72, pp. 29-47, 2021.

[18] A. Janeczek, J. Tomków, H. A. Derazkola, K. Łyczkowska, and D. Fydrych, "Effect of Underwater Friction Stir Welding Parameters on AA5754 Alloy Joints: Experimental Studies," The International Journal of Advanced Manufacturing Technology, vol. 134, pp. 5643-5655, 2024.

[19] B. Wang, L. Yu, M. Li, J. Guo, C. Ji, and J. Hu, "Welding Process Parameters and Mechanical Properties of Carbon Fiber-Reinforced Thermoplastic Composites: Experimental and Simulation Analysis," Engineering Fracture Mechanics, vol. 315, article no. 110831, 2025.

[20] W. Sun, H. Ma, and W. Qu, "A Hybrid Numerical Method for Non-Linear Transient Heat Conduction Problems with Temperature-Dependent Thermal Conductivity," Applied Mathematics Letters, vol. 148, article no. 108868, 2024.

[21] M. P. Iqbal, R. Jain, S. K. Pal, and P. Mandal, "Numerical Modelling of Friction Stir Welding of Pipes: Effect of Tool Shoulder on Mechanical Property and Metallurgical Characterization," Journal of Manufacturing Processes, vol. 79, pp. 326-339, 2022.

[22] P. Liu, Y. Cai, C. Du, Y Chen, Z. Zhao, and C. Zhang, "An Elastoplastic Mechanical-Thermal Model for Temperature Rise Simulation of Two-Dimensional Triaxially Braided Composites Under Quasi-Static Loads," Composite Structures, vol. 306, article no. 116559, 2023.

[23] R. Ghorbel, A. Ktari, and N. Haddar, "Experimental Analysis of Temperature Field and Distortions in Multi-Pass Welding of Stainless Cladded Steel," The International Journal of Advanced Manufacturing Technology, vol. 113, pp. 3525-3542, 2021.

[24] I. Šantak, A. Barac, M. Holik, and M. Živić, "Python-Based Calculation and Display of Temperature Field Distribution in Arc Welding," 12th International Scientific and Professional Conference SBZ, Engineering Technologies in Manufacturing of Welded Constructions and Products, Slavonski Brod, Požega, Croatia, 2023.

[25] L. E. de S. Paes, J. R. Andrade, F. S. Lobato, E. de S. Magalhães, V. Ponomarov, F. J. de Souza, et al., "Sensitivity Analysis and Multi-Objective Optimization of Tungsten Inert Gas (TIG) Welding Based on Numerical Simulation," The International Journal of Advanced Manufacturing Technology, vol. 122, pp. 783-797, 2022.

[26] M. D. Iordache, C. Badulescu, M. Diakhate, M. A. Constantin, E. L. Nitu, Y. Demmouche, et al., "A Numerical Strategy to Identify the FSW Process Optimal Parameters of a Butt-Welded Joint of Quasi-Pure Copper Plates: Modeling and Experimental Validation," The International Journal of Advanced Manufacturing Technology, vol. 115, pp. 2505-2520, 2021.

[27] D. K. Gupta and R. S. Mulik, "Thermo-Mechanical Modeling and Experimental Validation of Residual Stresses in ER70S-6 Component Manufactured by WAAM Process," Welding in the World, vol. 69, pp. 3351-3369, 2025.

[28] M. A. Afabor, E. Emozino, I. D. Friday, O. O. David, and A. S. Adzor, "Predictive Modelling of TIG Welding Process Parameters: A Comparative Study of Taguchi, Fuzzy Logic, and Response Surface Methodology," Nigerian Journal of Technology, vol. 44, no. 1, pp. 48-56, 2025.



Copyright© by the authors. Licensee TAETI, Taiwan. This article is an open-access article distributed under the terms and conditions of the Creative Commons Attribution (CC BY-NC) license (https://creativecommons.org/licenses/by-nc/4.0/).